



Contents lists available at ScienceDirect

Ad Hoc Networks

journal homepage: www.elsevier.com/locate/adhoc

Energy-efficient mobile relay deployment scheme for cellular relay networks

Hongbin Chen*, Wangfeng Chen, Feng Zhao

School of Information and Communication, Guilin University of Electronic Technology, Guilin 541004, China

ARTICLE INFO

Article history:

Received 21 July 2015

Revised 31 May 2016

Accepted 2 August 2016

Available online xxx

Keywords:

Cellular relay networks

Energy efficiency

Spectral efficiency

Mobile relay deployment

Interference graph

ABSTRACT

In this paper, an efficient mobile relay deployment scheme to select the deployment sites for mobile relay stations (MRSs) from the candidate positions is proposed, aiming at maximizing energy efficiency (EE) while guaranteeing the spectral efficiency (SE) requirement and the coverage constraints of mobile users (MUs). Firstly, an interference graph construction method is proposed to calculate the interference at MUs served by MRSs. Then, the deployment scheme at each observation time is proposed and our framework consists of three main algorithms. The first algorithm based on the extended Hungarian deployment algorithm is proposed to find the optimal solution, i.e., minimum movement distance. In addition, a greedy deployment algorithm and a static deployment algorithm are proposed to compare with the extended Hungarian deployment algorithm. Furthermore, we compare the performance of these algorithms via simulations and analyze the impact of various parameters on the performance. Simulation results demonstrate that the extended Hungarian deployment algorithm can considerably improve system EE compared to the other two algorithms. Moreover, relay switching occurs more frequently and average relay service time reduces with the increase of maximum speed of MUs.

© 2016 Published by Elsevier B.V.

1. Introduction

Recently, green cellular network has drawn great attention and investigation. It was estimated that the information and communication technology industry has contributed to about 2% of global CO₂ emissions and the energy consumed by base stations (BSs) accounts for about 60%–80% of the total network energy consumption [1]. Energy consumption in cellular networks has become an urgent problem to be solved and energy-efficient cellular networks will be a mainstream of future research. In order to handle this problem and improve network performance, the potential solution is to create heterogeneous networks by introducing other kinds of nodes in traditional cellular networks [2], such as pico BSs, femto BSs, and relay stations (RSs).

The relaying technology was once considered to be energy-efficient. The introduction of RSs between the BS and MUs can reduce transmission distance and improve throughput. But we must recognize that, more RSs deployed in cellular networks will bring higher energy consumption. Therefore, it is necessary to study and analyze the impact of deployment of RSs on the system performance.

At present, the investigation of RSs is mainly focused on the deployment of fixed RSs, which can extend the coverage and enhance the throughput. Once fixed RSs are deployed, their positions are no longer change. Many literatures have studied the influence of different deployment parameters on system performance. In [3], the authors proposed closed-form capacity expressions for interference-limited relay channels and used the expressions to determine the capacity of the cellular network, as well as the optimal position and number of relays that maximize the capacity. The problem of optimally placing relay nodes in a cellular network with the aim of maximizing the cell capacity in case of uniform and non-uniform traffic was addressed in [4]. In [5], joint deployment of BSs and RSs that trying to maximize the network capacity under the deployment cost and the coverage constraint was addressed. The authors proved that the problem is NP-hard and proposed a two-stage BS and RS deployment algorithm to obtain sub-optimal strategies. A similar idea was presented in [6], in which the authors proposed a novel cluster-based RS deployment scheme to select the appropriate deployment positions for the RSs from the candidate positions, considering the tradeoff among the network throughput, the deployment cost, and the overall coverage of the system. The authors in [7] considered a throughput-maximizing RS placement problem and formulated this problem as an integer linear programming (ILP). They proved that this problem is NP-hard and proposed a greedy heuristic to provide

* Corresponding author.

E-mail addresses: chbscut@guet.edu.cn (H. Chen), 857208202@qq.com (W. Chen), zhaofeng@guet.edu.cn (F. Zhao).

a sub-optimal solution to this problem. The authors in [8] studied the distance-aware RS placement problem in WiMAX mesh networks and presented two approximation algorithms to strategically deploy the minimum number of RSs in order to meet system requirements such as user data rate requests, signal quality, and network topology. For the deployment of multiple relays, the optimal positions of relays were studied for maximizing the reach to the destination subject to the quality-of-service requirement in [9].

In these works, the capacity and coverage performance of relay-assisted cellular networks have been widely studied, while the energy consumption of relay-assisted cellular networks gets little attention. The authors in [10] analyzed system coverage and energy consumption, and proposed a novel cellular network deployment strategy to jointly optimize the density and transmission powers of BSs. The authors in [11] investigated energy-efficient RS deployment, which showed that introducing appropriate number of RSs into cellular networks with proper positions can improve EE without compromising throughput. The authors in [12] presented the cognitive capacity harvesting network, where RSs were deployed to help the data transmission of secondary users. The problem of RS placement was studied to meet both SE and EE constraints. In [13], the macrocell and ultra-dense small cell deployment strategies have been evaluated from the network SE and network EE perspectives, with extreme densification levels, including both indoor and outdoor scenarios.

The deployment of RSs in the above works is static. In the case of the effect of surrounding obstacles or busy durations, fixed RSs are unable to provide high link reliability. Therefore, there have been many research studies that introduced mobile relay nodes in wireless networks to improve system performance. In wireless sensor networks (WSNs), it is difficult to achieve a large data collection rate because sensors usually have limited energy and communication resources. Mobile nodes may also be used as relays [14] that forward data from source nodes to the BS. Several movement strategies for mobile relays have been studied in [15,16]. In order to address this issue, the authors in [14] investigated the throughput capacity of WSNs, where multiple mobile relays were deployed to collect data from static sensors and forward them to a static sink. They also pointed out that the transmission range and the interference have great impact on capacity gain. The authors in [15] proposed using low-cost disposable mobile relays to reduce the energy consumption of data-intensive WSNs, in which MRSs move to different positions and then remain stationary to forward data along the paths from the sources to the BS. They also considered energy consumed by moving mobile relays. The authors in [16] investigated how to deploy mobile sensor nodes with minimum movement to form a WSN that provides both target coverage and network connectivity.

Some earlier works have investigated the deployment of MRSs in cellular networks to improve system performance, in which the MRSs can be classified as mobile user acting as MRS [17–20], RS on vehicles [21], relay robots [22], and mobile nomadic RS [23]. The authors in [17] studied relay selection in multi-hop cellular networks (MCNs) and proposed two mobile relay selection schemes, in which an idle mobile user acts as a RS. In [18], relay selection and resource allocation algorithms were proposed for mobile relay-enhanced cellular networks, which revealed that data rate of the cell-edge users which are far away from the BS and have lower channel gains increases by using MRSs with the proposed algorithms. More importantly, the authors in [19] reported the first experimental field tests, which validated and quantified the benefits of multi-hop cellular networks provided by using MRSs over traditional cellular networks. It is worth mentioning that, the authors in [20] compared the difference between the cellular network architecture with mobile and fixed RSs as well as their performance gain. In terms of increased capacity, MRSs are more ad-

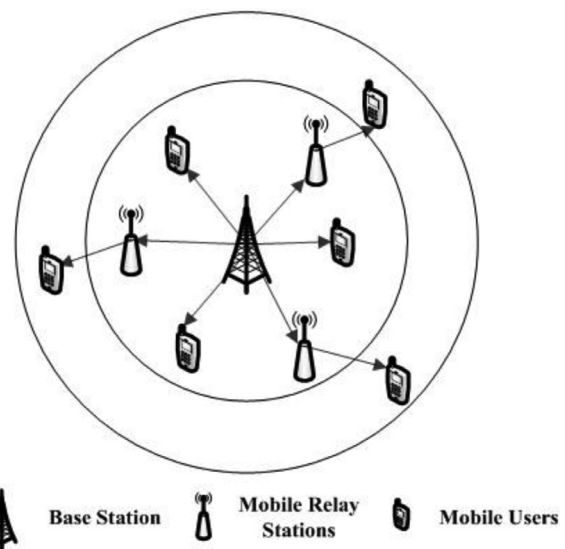


Fig. 1. Downlink transmission in a mobile relay-aided wireless cellular network.

vantageous than fixed RSs. Besides, the authors in [21] proposed an adaptive cost-based RS deployment approach to deploy various types of RSs: fixed RSs, nomadic RSs, and mobile RSs, which indicated that the transmission quality and service quality were increased by adding more RSs. In [22], the fundamental problem of finding optimal positions and allocation of relay robots to establish immediate end-to-end wireless communication in an inaccessible or dangerous area was addressed. Our work is inspired by the work in [23], in which the authors defined and studied the minimum mobile relay path selection problem, whose objective is to deploy minimum number of nomadic MRSs to patrol fixed RSs according to their busy durations. The fixed RSs' busy durations were predicted by using Markov chains, which were represented as a weighted graph. The algorithms based on the principles of graph searching, maximum matching, and maximum flow were proposed to solve the minimum vertex-disjoint path cover problem. But they ignored the energy consumed by moving mobile relays and did not consider the positions of MRSs.

To our knowledge, the EE maximization problem for MRS-aided cellular networks has not been well addressed in literature. Motivated by the above literature and inspired by Liao's work [23], referring to interference analysis in [24] and [25], we firstly analyze the interference at MUs by using the interference graph construction method. Then, in order to maximize the EE at each observation time, we propose an efficient mobile relay deployment scheme in the cellular relay network to select the deployment sites for MRSs from the candidate positions by taking into account the coverage constraints of MUs and the SE requirement.

The remainder of this paper is organized as follows. The system model is described in Section 2. In Section 3, an interference graph construction method is used to analyze the interference at MUs served by MRSs. Furthermore, the MRS deployment scheme and three deployment algorithms are proposed in Section 4. In Section 5, simulation results are presented, followed by some concluding remarks in Section 6.

2. System model

We consider a downlink, two-hop, mobile relay-aided wireless cellular network as shown in Fig. 1. We focus on a single cell with radius R . The BS is located at the center with coordinate $(0, 0)$. The cell is divided into two parts, that is, the inner circle with radius r_0 and the outer ring. At the initial observation time $t = 0$,

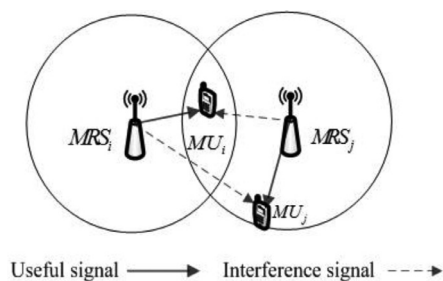


Fig. 2. Interference scenario between two MRSs.

a set of N MUs are uniformly distributed in the cell, which are denoted by $U = \{MU_1, MU_2, \dots, MU_N\}$. A set of M candidate MRSs are randomly distributed in the inner circle, which are denoted by $F = \{MRS_1, MRS_2, \dots, MRS_M\}$. The MUs in the inner circle directly communicate with the BS and the MUs in the outer ring communicate with the BS with the assistance of MRSs. In addition, in order to allow MUs to access the network anywhere and anytime, we also assume that the number of candidate MRSs is greater than the number of MUs, i.e., $M > N$. That is to say the MRSs in the cell form a virtual ultra-dense random distribution [13]. Actually, the observation time refers to the time instant when a MU resides in the outer ring and a MRS is deployed to serve it. For the ease of discussion, in the context the observation time refers to the time instant when all the MUs reside in the outer ring simultaneously. We assume that the MRSs and MUs reside in an obstacle-free environment, so that they can move in the cell freely.

All the stations are assumed to be half-duplex and have a single antenna [24]. The transmission powers of the BS and the MRSs are fixed. Each MRS is allowed to connect one MU only at any time but the BS is allowed to connect many MUs at the same time. The decode-and-forward relaying protocol is adopted and no signal combination at the receiver is done. The BS and the MRSs transmit in two non-overlapping time slots. The system bandwidth used for the cell is W Hz [24]. For the ease of analysis, the direct link between the BS and the MUs that are associated with MRSs is neglected due to, for instance, the shadowing effects. In order to improve the SE we assume that all the MRSs use the same frequency band, thus simultaneous transmissions may cause interference among MRSs, in which interference calculation is described in the next section.

In Section 4, we will discuss the MRS deployment scheme in detail. However, this scheme is not limited to this cellular network. In the proposed scheme, the BS coordinates the MRS deployment and for that it requires the moving information of all the MUs. Therefore, we assume that all the MUs are equipped with a global positioning system (GPS). In addition, we assume that the BS can accurately acquire the MU's arrival time and positions, and notify the appropriate MRSs in advance to arrive at the right place before the outer ring MUs arrive, while the candidate MRSs, which are not notified, wait for the notification from the BS.

3. Interference modeling

To calculate the system throughput and the SE, we need to analyze the interference among MRSs first. Since the transmission powers of MRSs are relatively small, when the distance between a MRS and another MRS is relatively large, the interference between them will be very small. So we can determine the minimum interfering distance between the two MRSs by using the interference graph construction method, as illustrated in Fig. 2.

We consider the scenario in which MRS_i and MRS_j are located at $(0, 0)$ and $(d, 0)$. The coverage radius of the MRSs is denoted by R_r . The minimum distance between MRSs and MUs is denoted

Algorithm 1

Interference graph construction (IGC).

```

1: Initialization:  $\mathbf{R}$ : MRS set;  $W(G) = w(i, j)_{K \times K}$ ;  $K = |V|$ 
2: for  $i = 1$  to  $K$  do
3:   for  $j = 1$  to  $K$  do
4:     if  $V_i \in \mathbf{R}, V_j \in \mathbf{R}$  and  $d_{i,j} < d_{\min}$  then
5:        $w(i, j) = P_R d_j^{-\beta} |h_j|^2$ 
6:     else
7:        $w(i, j) = 0$ 
8:     end if
9:   end for
10: end for
11:  $l(i) = \text{sum}\{w(i, j)\}$ 

```

by R_{\min} . When a MU is located at (x, y) , the received power from MRS_i and MRS_j are calculated by

$$P_{r,i} = P_R d_i^{-\beta} |h_i|^2 = P_R (x^2 + y^2)^{-\beta/2} |h_i|^2, \quad (1)$$

$$P_{r,j} = P_R d_j^{-\beta} |h_j|^2 = P_R ((x-d)^2 + y^2)^{-\beta/2} |h_j|^2, \quad (2)$$

where P_R is the transmission power of MRSs, d_i (d_j) is the distance from MU_i to MRS_i (MRS_j), $|h_i|^2$, $|h_j|^2$ are exponentially distributed with mean 1 in the Rayleigh fading environment, respectively. Let the path-loss exponent be $\beta = 4$ and ignore the noise power σ^2 , the SINR of the MU_i served by MRS_i is calculated by

$$\text{SINR}_{i,j}(x, y) = \frac{P_{r,i}}{P_{r,j} + \sigma^2} \approx \frac{((x-d)^2 + y^2)^2 |h_j|^2}{(x^2 + y^2)^2 |h_i|^2}. \quad (3)$$

When the MUs move into the coverage area of MRS_i which is $A_i = \{(x, y) | (x^2 + y^2) \leq R_r^2\}$, the area-average channel state of the coverage region of MRS_i is calculated by

$$\begin{aligned} \bar{C}_i(A_i, i, j) &= \int_{R_{\min}}^{R_r} \int_0^{2\pi} E[\text{SINR}_{i,j}] r dr d\theta / S(A_i) \\ &= 1 + \frac{8d^2}{R_r^2 - R_{\min}^2} \ln \frac{R_r}{R_{\min}} - \frac{8d^4}{(R_r^2 - R_{\min}^2)^2}. \end{aligned} \quad (4)$$

Note that the value of $\bar{C}_i(A_i, i, j)$ is only related to the distance between two MRSs. Thus, by letting $\bar{C}_i(A_i, i, j) < \text{SINR}_{th}$, we can obtain the minimum interfering distance, which is calculated by

$$d_{\min} = \sqrt{(R_r^2 - R_{\min}^2) \left(4 \ln \frac{R_r}{R_{\min}} - \sqrt{16 \left(\ln \frac{R_r}{R_{\min}} \right)^2 + 1 - \text{SINR}_{th}} \right)} \quad (5)$$

According to the positions of MRSs, when the distance between any two MRSs is less than d_{\min} , we believe that there exists inevitable interference between MRSs. We assume that the number of deployment MRSs is K . The interference graph is constructed as follows. The vertex \mathbf{V} of the graph denotes a MRS or a MU, the edge set \mathbf{E} denotes strong interference between MRSs. The element $w(i, j)$ of the weight matrix \mathbf{W} denotes the value of interference. $G(\mathbf{V}, \mathbf{E}, \mathbf{W})$ is a directed interference graph. The interference graph construction method is listed in Algorithm 1.

4. Relay deployment scheme

At the initial observation time $t = 0$, we have N MUs in the cell with coordinates $((x_1, y_1), (x_2, y_2), \dots, (x_N, y_N))$ and velocities $((v_1, \theta_1), (v_2, \theta_2), \dots, (v_N, \theta_N))$, where (v_1, v_2, \dots, v_N) denotes their speeds and $(\theta_1, \theta_2, \dots, \theta_N)$ denotes their directions. The deployment of MRSs mainly aims at the outer ring MUs and the coordinates of the corresponding candidate MRSs are denoted by

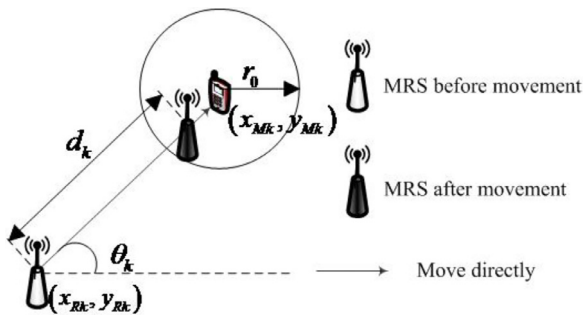


Fig. 3. Illustration of MRS movement.

$(x_{R1}, y_{R1}), (x_{R2}, y_{R2}), \dots, (x_{RM}, y_{RM})$. Since the MUs are always moving, the MU's positions at each observation time are different and the relay service time are different. So the number of deployed MRSs are different at each observation time. Nevertheless, this deployment scheme is applicable to every observation time.

As shown in Fig. 3, the transmission range of MUs is denoted by r_0 , i.e., the circle with a radius r_0 is MU's transmission range. If there exists MRSs in outer ring MU's transmission range, this outer ring MU will connect to only one MRS at a time. If there does not exist a MRS in an outer ring MU's transmission range, the BS will choose an appropriate MRS outside its transmission range to move to the right place. The MRSs are not always moving. They will move to the right place to provide services for the MUs only when they receive task notification from the BS. Otherwise, they will keep static.

We assume that the time required by a MU to move to a new position is T . After the BS acquires the MU's moving time and position, the BS informs the appropriate MRS to move to the right place within time T . Therefore, we think that the speed of the MRS does not need to be set, as long as the MRS can reach the right place within time T . However, the MU is constantly moving, only when the MRS falls within the MU's transmission range and the MRS can provide service for the MU. Otherwise, the BS will notify another suitable MRS to provide service for the MU. Let $d_{MB}(t)$ and $d_{MR}(t)$ denote the distance between the MU and the BS and the distance between the MRS and the MU at the time instant t , respectively. When the positions of MUs change, the following cases may occur, which lead to different results.

- (1) $d_{MB}(t) < r$: when the outer ring MU moves into the inner circle of the cell, the received signal of the MU from the BS is of good quality and may not require relaying. Therefore, the MU directly communicates with the BS.
- (2) $d_{MB}(t) > R$: when the outer ring MU moves out of the cell, it accesses to the BS in a neighboring cell.
- (3) $r \leq d_{MB}(t) \leq R$: when the MU in the neighboring cell or the inner circle of the cell moves into the outer ring of the cell, relay switching occurs. Here relay switching means the MU is associated with another MRS.
- (4) $d_{MR}(t) > r_0$ and $r \leq d_{MB}(t) \leq R$: when the MRS is not in the outer ring MU's transmission range and the outer ring MU is still in the outer ring, relay switching occurs.

As stated above, the conditions for relay switching are $r \leq d_{MB}(t) \leq R$; $r \leq d_{MB}(t) \leq R$, $d_{MR}(t) > r_0$. For ease of analysis, we assume that there are K MUs in the outer ring at the initial observation time $t = 0$. We only consider the movement of outer ring MUs and do not consider the inner circle MUs and MUs in neighboring cells.

The K outer ring MUs are denoted by two-dimensional coordinates $(x_{Mk}, y_{Mk}), k = 1, 2, \dots, K$ and velocities (v_{Mk}, θ_{Mk}) . We assume that the mobility models of all the outer ring MUs are ran-

dom walk, where v_{Mk} and θ_{Mk} are random variables following the uniform distribution, and $v_{Mk} \in [V_{\min}, V_{\max}]$, $\theta_{Mk} \in [0, 2\pi)$. Furthermore, the probability density functions (PDFs) of v_{Mk} and θ_{Mk} can be expressed as

$$f_V(v_{Mk}) = \begin{cases} \frac{1}{V_{\max} - V_{\min}}, & V_{\min} \leq v_{Mk} \leq V_{\max} \\ 0, & \text{other} \end{cases}, \quad (6)$$

$$f_{\Theta}(\theta_{Mk}) = 1/2\pi. \quad (7)$$

The positions of the MRSs for the K MUs are denoted by two-dimensional coordinates $(x_{Rk}, y_{Rk}), k = 1, 2, \dots, K$. Due to the energy consumption in the moving process and in order to reduce the handover of MRSs, a MRS should move along the straight line between its initial position and the position of target MU to minimize the movement distance, while satisfying the outer ring target MU coverage. Moreover, the MRS moves to the place $r_0/2$ far from the MU, in order to reduce handover. Let d_k denote the moving distance of k -th MRS. Then, $d_k = (x_{Mk} - x_{Rk})^2 + (y_{Mk} - y_{Rk})^2 - r_0/2$. θ_k denotes the MRS's moving direction. Let Δx_k and Δy_k denote the coordinate variables. We have $\Delta x_k = x_{Mk} - x_{Rk}$ and $\Delta y_k = y_{Mk} - y_{Rk}$. Because the MRS is moving along a straight line, θ_k can be easily obtained as follows:

- (1) $\Delta x_k > 0$ and $\Delta y_k > 0$, $\theta_k = \arctan(\frac{y_{Mk} - y_{Rk}}{x_{Mk} - x_{Rk}})$;
- (2) $\Delta x_k < 0$ and $\Delta y_k > 0$, $\theta_k = \arctan(\frac{y_{Mk} - y_{Rk}}{x_{Mk} - x_{Rk}}) + \pi$;
- (3) $\Delta x_k < 0$ and $\Delta y_k < 0$, $\theta_k = \arctan(\frac{y_{Mk} - y_{Rk}}{x_{Mk} - x_{Rk}}) + \pi$;
- (4) $\Delta x_k > 0$ and $\Delta y_k < 0$, $\theta_k = \arctan(\frac{y_{Mk} - y_{Rk}}{x_{Mk} - x_{Rk}}) + 2\pi$.

After the MRS moves a distance d_k with a certain speed, the new coordinate of the MRS is obtained as

$$\begin{aligned} x'_{Rk} &= x_{Rk} + d_k \cos \theta_k \\ y'_{Rk} &= y_{Rk} + d_k \sin \theta_k. \end{aligned} \quad (8)$$

Since the MUs are constantly moving, when the positions of MUs change, their respective coordinates change to (x'_{Mk}, y'_{Mk}) after time t_{Mk} , where $x'_{Mk} = x_{Mk} + v_{Mk} t_{Mk} \cos \theta_{Mk}$, $y'_{Mk} = y_{Mk} + v_{Mk} t_{Mk} \sin \theta_{Mk}$. Note that when the distance between the MU and the MRS is r_0 , relay switching occurs. Therefore, we have

$$d_{MRk}(t_{Mk}) = r_0. \quad (9)$$

The expression of $d_{MRk}(t_{Mk})$ is obtained as

$$d_{MRk}(t_{Mk}) = \sqrt{(x'_{Mk} - x_{Rk})^2 + (y'_{Mk} - y_{Rk})^2}. \quad (10)$$

Using (9) and (10), we obtain

$$\begin{aligned} t_{Mk} &= -\frac{(x_{Mk} \cos \theta_{Mk} + y_{Mk} \sin \theta_{Mk} - x_{Rk} \cos \theta_{Mk} - y_{Rk} \sin \theta_{Mk})}{v_{Mk}} \\ &+ \frac{\sqrt{r_0^2 - (x_{Mk} \sin \theta_{Mk} - y_{Mk} \cos \theta_{Mk} - x_{Rk} \sin \theta_{Mk} + y_{Rk} \cos \theta_{Mk})^2}}{v_{Mk}}. \end{aligned} \quad (11)$$

Since the moving speeds and directions of MUs are different, the MRS's service time may be the same or different. When the MRS is not in the outer ring MU's transmission range, the MRS becomes idle and waits for the next mission. We assume that the time of MU need MRS to service t_{need} is a random variable, which satisfies the exponent distribution with mean value $1/\lambda$ [17]. The PDFs of t_{need} can be expressed as

$$f_T(t_{need}) = \begin{cases} \lambda e^{-\lambda t_{need}}, & t_{need} > 0 \\ 0, & \text{other.} \end{cases} \quad (12)$$

When the MRS is not in the MU's transmission range, relay switching occurs. The probability of occurrence of relay switching is expressed as

$$P_{\text{handover}} = P(t_{\text{need}} > t_{Mk}) \\ = \int_{t_{Mk}}^{\infty} \lambda e^{-\lambda t_{\text{need}}} dt_{\text{need}} = e^{-\lambda t_{Mk}}. \quad (13)$$

Therefore, the average relay switching rate is expressed as

$$E(P_{\text{handover}}) = \frac{1}{2\pi(V_{\text{max}} - V_{\text{min}})} \int_{V_{\text{min}}}^{V_{\text{max}}} \int_0^{2\pi} e^{-\lambda t_{Mk}} d\theta_{Mk} dv_{Mk}. \quad (14)$$

We define t_{ave} as the average value of t_{Mk} , i.e., average MRS's service time, which is

$$t_{\text{ave}} = \frac{1}{2\pi(V_{\text{max}} - V_{\text{min}})} \int_{V_{\text{min}}}^{V_{\text{max}}} \int_0^{2\pi} t_{Mk} d\theta_{Mk} dv_{Mk}. \quad (15)$$

According to the proposed scheme, the power consumption and the EE at each observation time are analyzed in the following. We adopt the distance-proportional energy consumption model which is appropriate for this kind of nodes [15]. The energy $E(d_k)$ consumed by moving a distance d_k is modeled as:

$$E(d_k) = \bar{k} d_k \cdot s_k, \quad (16)$$

where the value of the parameter \bar{k} depends on the speed of the MRS, and we assume it is a constant. s_k is a binary variable, which is defined as follows:

$$s_k = \begin{cases} 1, & \text{if MRS}_k \text{ moves a distance } d_k \\ 0, & \text{otherwise} \end{cases}. \quad (17)$$

At the initial observation time $t=0$, recall the downlink transmission as shown in Fig. 1. The transmission process is divided into two phases. In the first phase, the BS transmits signals to each associated MU or MRS. Then, the received signals at the corresponding MRSs and MUs are respectively represented by

$$z_k(t) = \sqrt{P_B d_{Rk}^{-\beta} |h_{Rk}|^2} x_k(t) + v_k(t), \quad k = 1, 2, \dots, K, \quad (18)$$

$$z_l(t) = \sqrt{P_B d_{Ml}^{-\beta} |h_{Ml}|^2} x_l(t) + v_l(t), \quad l = K+1, \dots, N, \quad (19)$$

where P_B is the transmission power of the BS, x_k and x_l are the signals transmitted by the BS (assuming that $E\{|x_k|^2\} = 1$, $E\{|x_l|^2\} = 1$, where $E\{\cdot\}$ is the expectation operator), d_{Rk} is the distance from BS to its associated MRS and d_{Ml} is the distance from the BS to its associated MU, $|h_{Rk}|^2$, $|h_{Ml}|^2$ are exponentially distributed with mean 1 in the Rayleigh fading environment, respectively, v_k and v_l are additive white Gaussian noises (AWGNs) with zero mean and variance σ^2 . In the second phase, the MRSs forward their decoded signals to the associated MUs. It is assumed that the decoding is always successful. The signals received at the corresponding MUs can be written as

$$y_k(t) = \sqrt{P_R d_{Mk}^{-\beta} |h_{Mk}|^2} x_k(t) + Q_k + w_k(t), \quad k = 1, \dots, K, \quad (20)$$

where d_{Mk} is the distance from a MRS to its associated MU, $|h_{Mk}|^2$ is exponentially distributed with mean 1 in the Rayleigh fading environment, w_k is an AWGNs with zero mean and variance σ^2 . Since interference is introduced by simultaneous transmissions from MRSs, Q_k denotes k -th MU which is associated with an MRS suffers interference from other MRSs, with variance I_k . Therefore, the SINRs at the MUs are

$$\gamma_k = \frac{P_R d_{Mk}^{-\beta} |h_{Mk}|^2}{\sigma^2 + I_k}, \quad k = 1, 2, \dots, K, \quad (21)$$

$$\gamma_l = \frac{P_B d_{Ml}^{-\beta} |h_{Ml}|^2}{\sigma^2}, \quad l = K+1, \dots, N. \quad (22)$$

Since we only consider the throughput perceived by the MUs, the cell throughput is given by

$$R = \frac{1}{2} W \sum_{k=1}^K \log_2(1 + \gamma_k) + \frac{1}{2} W \sum_{l=K+1}^N \log_2(1 + \gamma_l). \quad (23)$$

In order to quantify the energy consumption of the system, referring to [9], the power consumption of the BS and MRSs can be simply written as the linear form

$$P_{B,\text{tot}} = \Delta_B P_B + P_{B0}, \quad (24)$$

$$P_{R,\text{tot}} = \Delta_R P_R + P_{R0}. \quad (25)$$

where B and R represent the BS and MRSs, respectively. The coefficients Δ_B and Δ_R account for the power consumption that scales with the average radiated power due to amplifier and feeder losses as well as cooling of sites. The static powers P_{B0} and P_{R0} includes the one used for signal processing, battery backup, and cooling. The system SE is defined as

$$\eta_{SE} = \frac{1}{2} \sum_{k=1}^K \log_2(1 + \gamma_k) + \frac{1}{2} \sum_{l=K+1}^N \log_2(1 + \gamma_l). \quad (26)$$

The system EE is defined as

$$\eta_{EE} = \frac{\frac{1}{2} W \sum_{k=1}^K \log_2(1 + \gamma_k) + \frac{1}{2} W \sum_{l=K+1}^N \log_2(1 + \gamma_l)}{(\Delta_B P_B + P_{B0}) + K \cdot (\Delta_R P_R + P_{R0}) + \sum_{k=1}^K E_k(d_k)}. \quad (27)$$

Our target is to maximize the system EE while satisfying the η_{SE} requirement and the coverage constraints of MUs, which can be formulated as

$$\begin{aligned} \max \quad & \eta_{EE} \\ \text{s.t.} \quad & \eta_{SE} \geq \bar{\eta}_{SE}, \\ & d_{Mk} \leq r_0, \quad k \in (1, \dots, K), \end{aligned} \quad (28)$$

where $\bar{\eta}_{SE}$ is the minimum required SE.

In our deployment scenario, each outer ring MU can find its own MRS, that is to say, after MRSs are chosen and move to new positions, the distance between a MU and its associated MRS is known. When the positions of MRSs are fixed, the MU's interference suffering from other MRSs can be calculated by using the interference graph construction (IGC) method. When the MU determines the choice of the BS or a MRS, the cell throughput can be seen as a constant under the proposed deployment scheme at the observation time t . According to the expression of EE and based on the coverage constraint, if we want to maximize the EE, we just need to minimize the energy consumed by moving, i.e., to minimize the total movement distance.

When the MRSs move to new positions, it is possible that the distance between any two MRSs is very close. A MU will suffer high interference from the neighboring MRSs and its data rate will become low. According to the formula (26), this can cause lower SE under the large interference situations. Therefore, in order to improve SE under the existence of large interference, when $\eta_{SE} < \bar{\eta}_{SE}$, the MU that connected to a MRS and has minimum data rate directly communicates with the BS for interference reduction. Then, the MRSs are reassigned to the MUs, and we recalculate the interference and SE until $\eta_{SE} \geq \bar{\eta}_{SE}$.

Definition 1. Mobile Relay Deployment (MRD) problem: At the initial observation time $t=0$, given K outer ring target MUs with known positions and M candidate MRSs deployed randomly in the inner circle, move MRSs to new positions such that the target MUs are covered and the total movement distance of MRSs is minimized.

The MRD problem is also a target MU coverage problem (TCOV), and the TCOV is shown to be NP-hard [16]. Therefore, our problem is also NP-hard. Since each MRS is allowed to connect one MU

only, our MRD problem in this scenario could be transferred to the assignment problem that is to assign exactly one MRS to each target MU in such a way that the total movement distance is minimized. Next, the extended Hungarian algorithm is proposed to find the optimal solution to the MRD problem, i.e., which MRS should move and to which potential target MU, so as to cover the target MUs. In order to compare the performance of the extended Hungarian deployment algorithm, a sub-optimal greedy deployment algorithm and a static deployment algorithm are also proposed.

4.1. Extended Hungarian Deployment Algorithm (EHDA)

In the traditional assignment problem, the number of agents equals the number of tasks ($K = M$), while in our MRD problem, in order to ensure that the outer ring MUs are able to find suitable MRSs, the number of MRSs is usually larger than the number of MUs, i.e., $M > K$. Actually, at the initialization stage of the cellular network, a set of M candidate MRSs are randomly distributed in the inner circle and a set of N MUs are randomly distributed in the cell. We can find out the outer ring MUs according to their positions. May be some target MUs may have already been covered by MRSs, therefore, in Step 1, the SINRs of outer ring target MUs are calculated and sorted by $\gamma_1 < \gamma_2 < \dots < \gamma_K$. Then, in order to ensure the fairness of MUs, assuming that the first MU has the priority to choose the nearest MRS in its transmission range in Step 2. Denote the set of target MUs that have already been covered by K_{cov} , and denote the set of MRSs that cover these target MUs by M_{cov} . Denote the set of uncovered target MUs by K_{ucov} , and denote the set of rest MRSs by M_{ucov} . Then, we have $K_{ucov} = U \setminus K_{cov}$, $M_{ucov} = F \setminus M_{cov}$, that is to say we should remove the MU served by the chosen MRS from outer ring MU list and delete the MRS selected by MU from MRS list in Step 3, and then update the outer ring MU list and the MRS list in Step 4, until next. The number of K_{ucov} is assumed to be n , and the number of M_{ucov} is assumed to be m , $m > n$. To deal with this issue, we extended the Hungarian algorithm proposed in [16] by extending the cost matrix to an $m \times m$ matrix as follows:

$$[e_{\hat{i}, \hat{j}}]_{m \times m} = \begin{pmatrix} e_{1,1} & \dots & e_{1,n} & 0 & \dots & 0 \\ \vdots & & \vdots & \vdots & & \vdots \\ e_{m,1} & \dots & e_{m,n} & 0 & \dots & 0 \end{pmatrix}$$

where $e_{\hat{i}, \hat{j}}$ ($1 \leq \hat{i} \leq m$, $1 \leq \hat{j} \leq n$) is set as the movement distance of moving $MRS_{\hat{i}}$ to cover target $MU_{\hat{j}}$, i.e.,

$$e_{\hat{i}, \hat{j}} = \begin{cases} d(MRS_{\hat{i}}, MU_{\hat{j}}) - r_0/2, & \text{if } d(MRS_{\hat{i}}, MU_{\hat{j}}) > r_0 \\ 0, & \text{otherwise} \end{cases}$$

where $d(MRS_{\hat{i}}, MU_{\hat{j}})$ is the Euclidean distance between $MRS_{\hat{i}}$ and $MU_{\hat{j}}$. In Step 5, with the extended cost matrix, the optimal solution to the MRD problem can be obtained by using the Hungarian algorithm. After the outer ring MUs have selected suitable MRSs, we calculate SE in Step 6. If SE is not greater than or equal to the minimum required SE, we execute Step 7, and then go back to Step 2. The MRSs are reassigned to the MUs, until the SE is greater than or equal to the minimum required SE. The extended Hungarian deployment algorithm (EHDA) is summarized in Fig. 4.

From Steps 1 to 4, the computational complexity is about $O(KM)$. As for the extended Hungarian algorithm, a $m \times m$ cost matrix is constructed. Hence the computational complexity of the extended Hungarian algorithm is $O(m^3)$ [16]. So the total computational complexity of the extended Hungarian deployment algorithm is $O(KM+m^3)$.

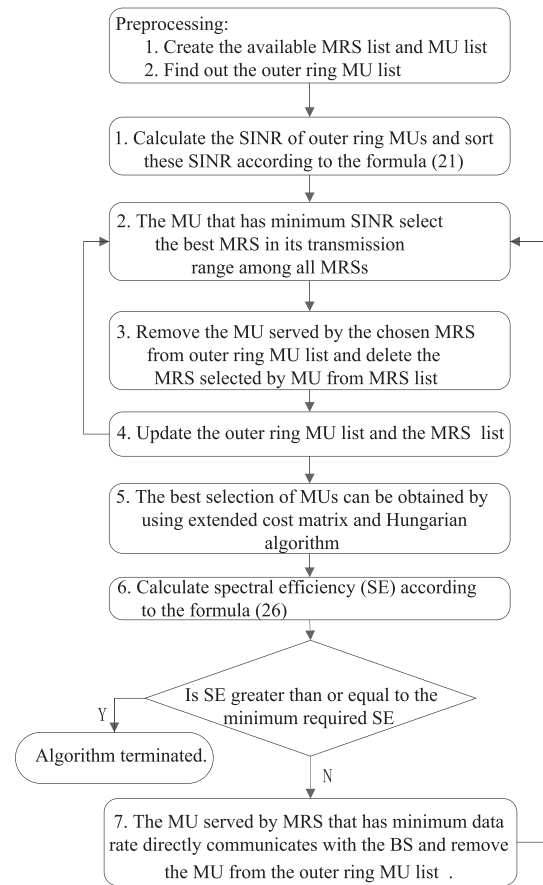


Fig. 4. Flow chart of the EHDA.

4.2. Greedy deployment algorithm (GDA)

The EHDA and GDA are all the same from initialization to Step 4. The difference between them is in Step 5. Given K target MUs and M MRSs, some target MUs may have been covered at the initialization. Therefore, the SINRs of all outer ring target MUs are sorted by $\gamma_1 < \gamma_2 < \dots < \gamma_K$, in order to ensure the fairness of MUs, assuming that the first MU has the priority to choose the nearest MRS in its transmission range, until next. These steps can be found in the flow chart of the EHDA, so we will not repeat them and only focus on Step 5. When some of the outer ring target MUs find the appropriate MRSs, we just need to think about the uncovered MUs. Then, in Step 5, the SINRs of outer ring uncovered target MUs are sorted by $\gamma_1 < \gamma_2 < \dots < \gamma_n$, and the MUs choose the appropriate MRSs one by one. The first MU has the priority to choose the nearest MRS which is not in this MU's transmission range, and then the MRS should move along the straight line between its initial position and the position of this MU to minimize the movement distance. Next the second MU will choose the nearest MRS from the rest MRSs, and so on. The sub-optimal solution to the MRD problem can be obtained by using the greedy deployment algorithm.

From Steps 1 to 4, the computational complexity is $O(KM)$. In Steps 5 of the greedy deployment algorithm, the computational complexity is $O(nm)$. So the total computational complexity of the greedy deployment algorithm is $O(KM+nm)$.

4.3. Static deployment algorithm (SDA)

The EHDA and SDA are all the same from initialization to Step 4. The difference between them is also in Step 5. The static

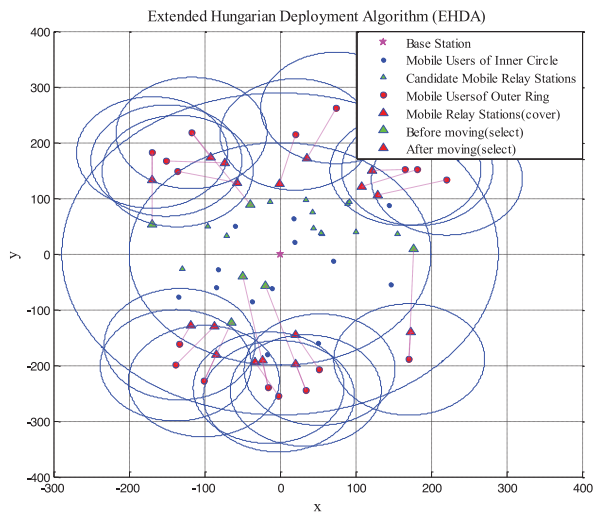


Fig. 5. Illustration of a deployment example of EHDA.

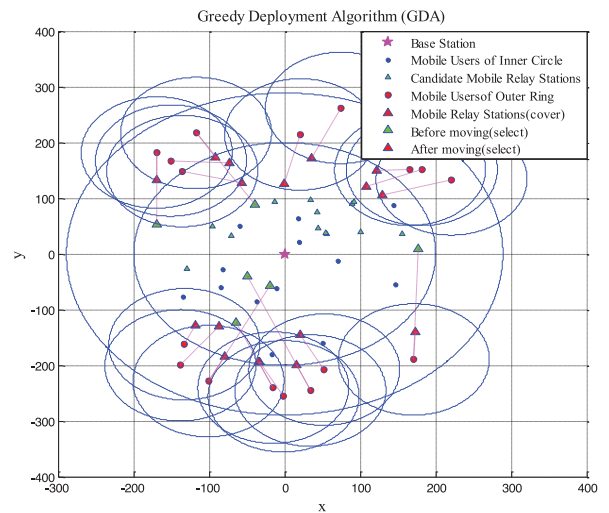


Fig. 6. Illustration of a deployment example of GDA.

deployment algorithm is designed following the static deployment schemes in wireless sensor networks. Given K outer ring target MUs and M MRSs, some target MUs may have been covered at the initialization. The SINRs of outer ring target MUs are sorted by $\gamma_1 < \gamma_2 < \dots < \gamma_K$. The MUs choose the appropriate MRSs one by one. The first MU has the priority to choose the nearest MRS. If there exists MRSs in the MU's transmission range, the MU will choose the nearest MRS. Next the second MU will choose the nearest MRS that in the MU's transmission range from the rest MRSs, and so on. These steps can also be found in the flow chart of the EHDA, so we will not repeat them and focus on Step 5. Because there do not exist MRSs in the MU's transmission range for the outer ring uncovered target MUs, then, in Step 5, these outer ring uncovered MUs directly communicate with the BS. The MRSs do not move in the whole deployment process.

From Steps 1 to 4, the total computational complexity of the static deployment algorithm is $O(KM)$.

5. Performance evaluation

In this section, we evaluate the performance of the proposed three algorithms by using the MATLAB tool. The inter-site distance between the neighboring cells is defined as an LTE standard distance of 500 m, with a cell radius $d_{\min}=0$ of 289 m [17]. The transmission distance r_0 is 100 m, the radius of MRSs R_r is 100 m, and the minimum distance between MRSs and MUs R_{\min} is 10 m. All the MUs are uniformly distributed in the cell and move randomly. The speeds of the MUs randomly take values between 0 m/s and 5 m/s. The directions of the MUs randomly take values in the interval $[0, 2\pi)$. A MRS moves along the straight line between its initial position and the position of the target MU. Since we assume the MRSs can reach the right place within the time T , the speeds of the MRSs are not set. In practice, the speeds of the MRSs can be set according to actual situations. The power consumption parameters are set as $P_B = 2W$, $\Delta_B = 1/0.38$, $P_{B0} = 1W$, $P_R = 0.2W$, $\Delta_R = 1/0.38$, $P_{B0} = 0.1W$, $k = 2W/km$. The average service time λ is 100 s. The parameters of path-loss exponent, noise power, total bandwidth, and minimum required SE are set to 4, -50 dBm, 10 kHz, and 5 bps/Hz, respectively.

Figs. 5–7 show the deployment results of the EHDA, the GDA, and the SDA, respectively, when the number of candidate positions for the MRSs is 30 and the number of MUs is also 30. It can be observed that the MRSs in the MUs transmission range and are chosen by the MUs are the same for the EHDA, the GDA, and the SDA

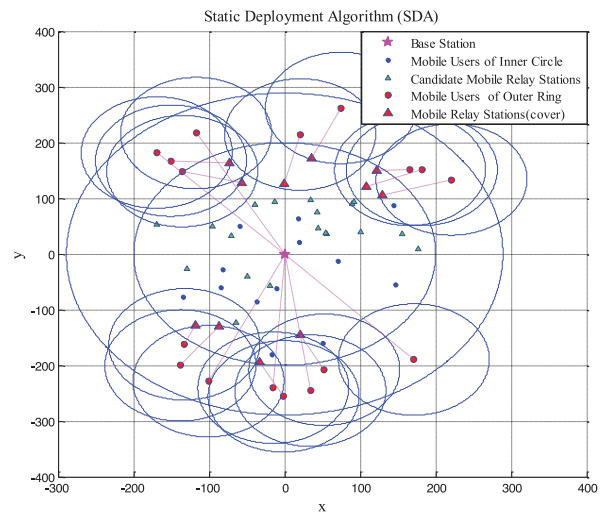


Fig. 7. Illustration of a deployment example of SDA.

under the same coverage constraint. As Figs. 5 and 6 show, for the EHDA and the GDA, some of the MRSs are chosen by the MUs that do not have MRSs in their transmission range and the results are different. It is because the deployment rules of the EHDA and the GDA are different, so the MRSs chosen by the MUs are different. The entire outer ring MUs can be covered by chosen MRSs for the EHDA and the GDA. Fig. 7 shows that the MU that does not have a MRS in its transmission range directly communicates with the BS and the MRSs in the MUs' transmission range will be notified to provide service for the MUs.

According to Figs. 6 and 7, under the same coverage constraint, the moving paths of MRSs are different and the distances are also different for the EHDA and the GDA. As shown in Fig. 8, when the number of candidate positions for the MRSs is small, the total movement distance with the EHDA is less than the total movement distance with the GDA. The reason for this result is that the EHDA is the optimal algorithm which can find the minimum total movement distance, while the GDA is the heuristic sub-optimal solution. Moreover, when the number of candidate positions of MRSs increases, the total movement distances decreases. The reason for this result is that when the number of candidate positions of MRSs increases, the probability of the event that the number of MRSs located in each outer ring MU's transmission range will be large, i.e., the MUs can find their MRSs in the transmission range, and the

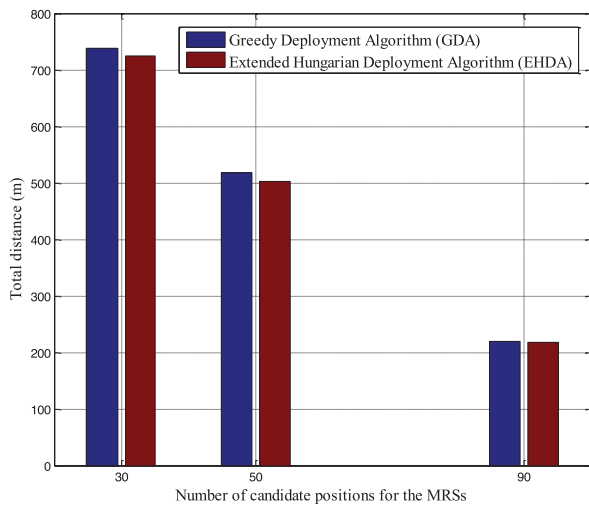


Fig. 8. Total movement distance versus number of MRSs (number of MUs is 30).

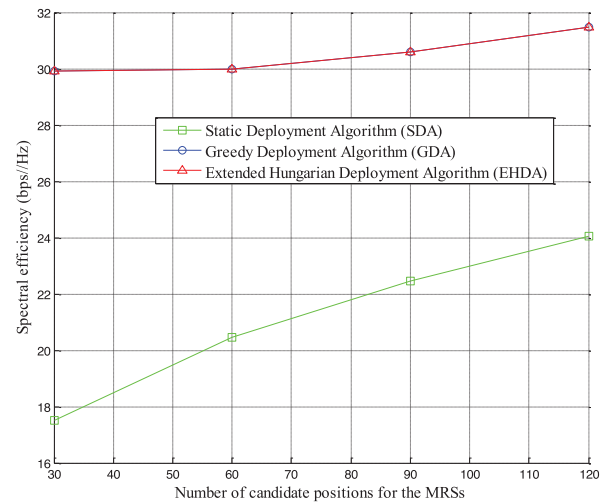


Fig. 10. Spectral efficiency versus number of MRSs.

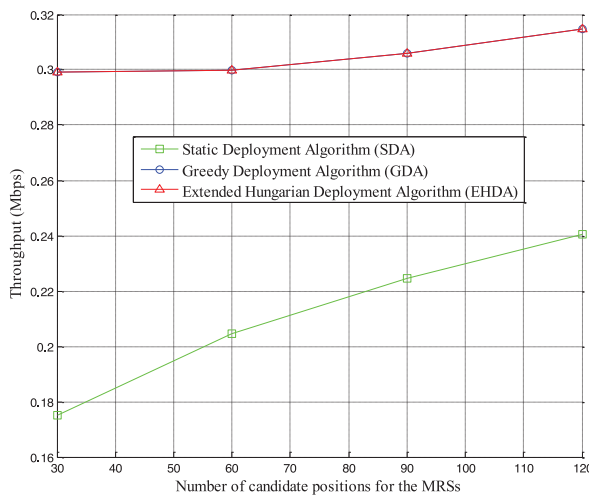


Fig. 9. Cell throughput versus number of MRSs.

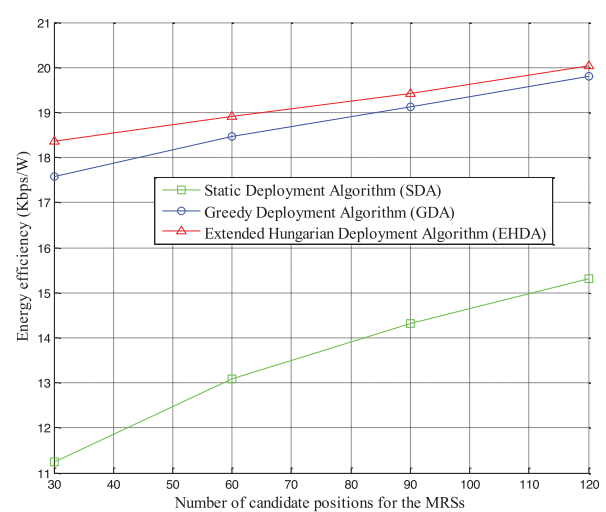


Fig. 11. Energy efficiency versus number of MRSs.

MRSs do not need to move to cover the MUs. In addition, when the number of candidate positions of MRSs is relatively large, the total movement distance with the EHDA and the GDA are very close to each other.

Figs. 9–11 show the cell throughput, SE, and EE versus the number of MRSs when the number of MUs is 30 and the SINR threshold is 0 dB. When the SINR threshold is 0 dB, according to the IGC method, we have $d_{\min} = 0$, which means that there does not exist interference between any two MRSs. Under the same coverage constraint, the throughput and the SE with the GDA and the ones with the EHDA is the same, but better than those with SDA in Figs. 9 and 10. In addition, the EE with the EHDA is greater than the one with the GDA and the SDA. As shown in Fig. 11, we can see that the gap between that with the EHDA and the one with the GDA decreases when the number of candidate positions of MRSs increases. It is because the total movement distance decreases when the number of candidate positions of MRSs increases. When the number of candidate positions of MRSs is relatively large, the total movement distance with the EHDA and the GDA are very close to each other. Furthermore, when the number of candidate positions of MRSs increases, the probability of the event that the number of MRSs located in each outer ring MU's transmission range will be large, and the MUs can find their MRSs in the transmission range. The distance between the MU and the MRS will become smaller,

hence the throughput, SE, and EE increases with the number of candidate positions of MRSs.

Figs. 12–14 show the effect of SINR threshold on the system performance when the number of candidate positions for the MRSs is 30 and the number of MUs is also 30. First, in Fig. 12, we can observe that the cell throughput with the SDA is significantly less than those with the GDA and the EHDA, and the cell throughput with the GDA is greater than that with the SDA and is similar to that with the EHDA. It is worth pointing out that the result with the GDA and with the EHDA is the same in terms of throughput and SE when the SINR threshold changes. For the SDA, the SE can meet the minimum SE requirement under our deployment scheme, as shown in Fig. 13. Moreover, the EHDA achieves the highest EE, while the SDA achieves the lowest, as shown in Fig. 14. The reason is that the total movement distance is different with the GDA and the EHDA, thus the energy consumed in the moving process is different. Under the same coverage constraint, the total movement distance and the energy consumed with the EHDA is the minimum. Moreover, we can observe that higher SINR threshold leads to worse performance of the system. It is because, when the SINR threshold increases, according to the IGC method, the minimum interference distance increases, which means that the probability of interference between any two

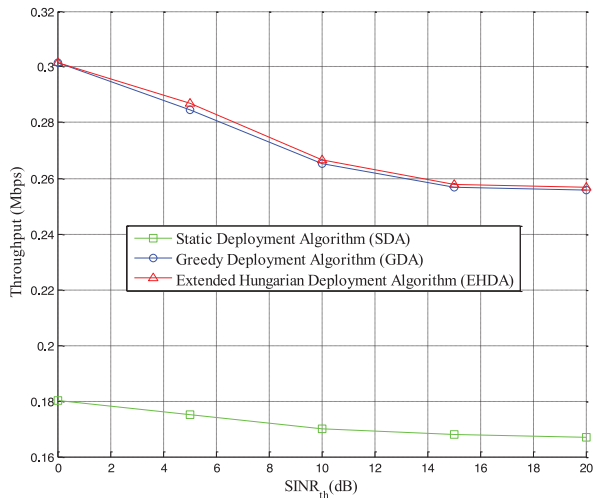


Fig. 12. Cell throughput versus SINR threshold.

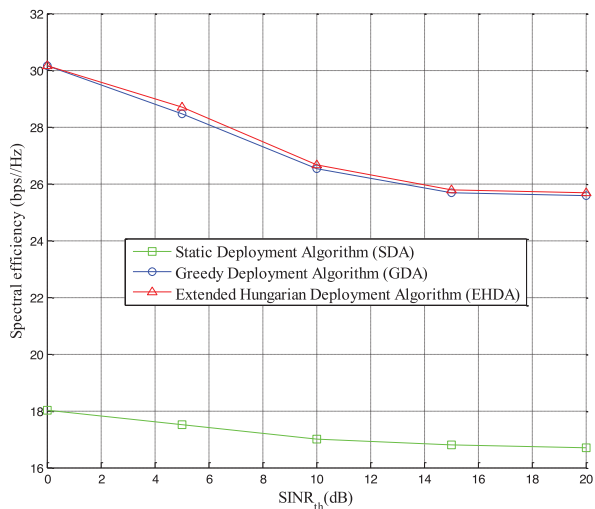


Fig. 13. Spectral efficiency versus SINR threshold.

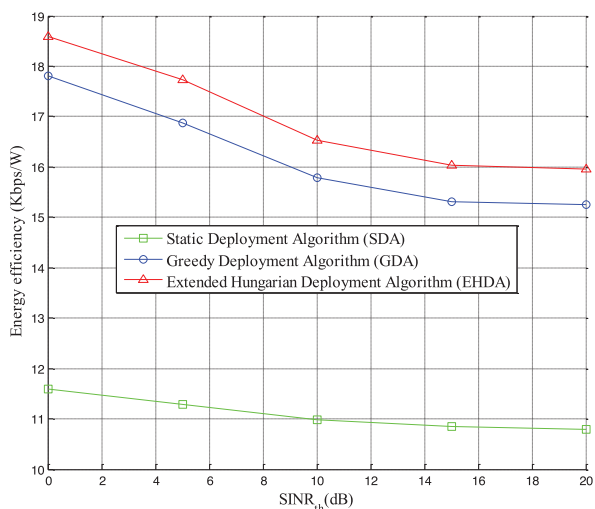


Fig. 14. Energy efficiency versus SINR threshold.

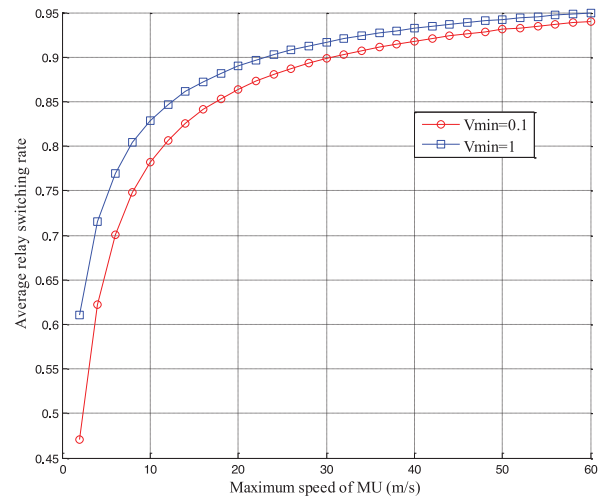


Fig. 15. Effect of maximum MU speed on average relay switching rate.

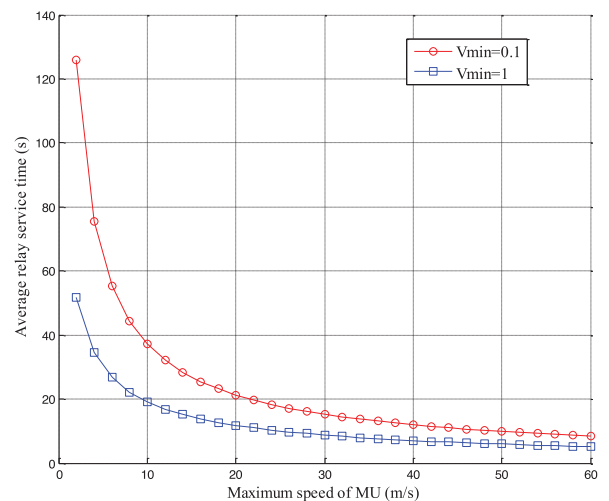


Fig. 16. Effect of maximum MU speed on average relay service time.

MRSs also increases. The greater interference will result in smaller throughput.

Figs. 15 and 16 show the effect of maximum MU speed V_{\max} on average relay switching rate and average relay service time, respectively. With the increase of the maximum MU speed, the average relay switching rate increases while the average relay service time reduces. The reason is that when the MU speed increases, relay switching occurs more frequently. Subsequently, we can also infer that in the case of minimum MU speed V_{\min} , the average relay switching rate will decrease and the average relay service time will increase.

6. Conclusion

In this paper, the impact of MRS deployment on the performance of a cellular relay network is studied. Specifically, the EE-maximizing MRS deployment problem at each observation time is mathematically formulated. Considering the coverage constraints of MUs and the SE requirement, we first calculate the interference at MUs served by MRSs based on the IGC method, and then propose three deployment algorithms to maximize the EE, i.e., to minimize the total movement distance. The complexity of the three deployment algorithms is analyzed. Then, the impact of the number of candidate positions of MRSs and the SINR threshold on the performance are investigated. The effect of maximum MU speed

on average relay switching rate and average relay service time are also discussed. Simulation results demonstrate the superior performance of EHDA in terms of the total movement distance as well as the system EE. In addition, higher maximum MU speed will lead to higher average relay switching rate and shorter average relay service time.

Acknowledgment

This research was supported by the National Natural Science Foundation of China (61162008, 61172055, 61471135), the Guangxi Natural Science Foundation (2013GXNSFGA019004, 2015GXNSFBB139007), and the Innovation Project of Guangxi Graduate Education (YCSZ2015144).

References

- [1] L. Suarez, L. Nuaymi, J. Bonnin, An overview and classification of research approaches in green wireless networks, *EURASIP J. Wirel. Commun. Netw.* 2012 (Apr. (13)) (2012) 1–18.
- [2] Y.S. Soh, T.Q.S. Quek, M. Kountouris, H. Shin, Energy efficient heterogeneous cellular networks, *IEEE J. Sel. Areas Commun.* 31 (5) (May 2013) 840–850.
- [3] W. Guo, T. O'Farrell, Relay deployment in cellular networks: planning and optimization, *IEEE J. Sel. Areas Commun.* 31 (Aug. (8)) (2013) 1597–1606.
- [4] M. Minelli, M. Ma, M. Coupechoux, J.-M. Kelif, M. Sigelle, P. Godlewski, Optimal relay placement in cellular networks, *IEEE Trans. Wireless Commun.* 13 (Feb. (2)) (2014) 998–1009.
- [5] H.-C. Lu, W. Liao, Joint base station and relay station placement for IEEE 802.16j networks, in: *Proc. IEEE GLOBECOM*, Nov.–Dec. 2009, pp. 1–5.
- [6] J.Y. Chang, Y. Chen, A cluster-based relay station deployment scheme for multi-hop relay networks, *J. Commun. Netw.* 17 (Feb. (1)) (2015) 84–92.
- [7] H. Lu, W. Liao, F. Lin, Relay station placement strategy in IEEE 802.16j WiMAX networks, *IEEE Trans. Commun.* 59 (Jan. (1)) (2011) 151–158.
- [8] W. Zhang, S. Bai, G. Xue, J. Tang, C. Wang, DARP: distance aware relay placement in WiMAX mesh networks, in: *Proc. INFOCOM*, Apr. 2011, pp. 2060–2068.
- [9] X. Li, D. Guo, J. Grosspietsch, H. Yin, G. Wei, Maximizing mobile coverage via optimal deployment of base station and relays, *IEEE Trans. Veh. Tech.* 65 (Jul. (19)) (2016) 5060–5070.
- [10] J. Peng, P. Hong, K. Xue, Energy-aware cellular deployment strategy under coverage performance constraints, *IEEE Trans. Wireless Commun.* 14 (Jan. (1)) (2015) 69–80.
- [11] G. Wu, G. Feng, Energy-efficient relay deployment in next generation cellular networks, in: *Proc. IEEE ICC*, Jun. 2012, pp. 5757–5761.
- [12] H. Yue, M. Pan, Y. Fang, S. Glisic, Spectrum and energy efficient relay station placement in cognitive radio networks, *IEEE J. Sel. Areas Commun.* 31 (May. (5)) (2013) 883–893.
- [13] S. Yunas, M. Valkama, J. Niemela, Spectral and energy efficiency of ultra-dense networks under different deployment strategies, *IEEE Commun. Mag.* 53 (Jan. (1)) (2015) 90–100.
- [14] W. Liu, K. Lu, J. Wang, L. Huang, D. Wu, On the throughput capacity of wireless sensor networks with mobile relays, *IEEE Trans. Veh. Tech.* 61 (May. (4)) (2012) 1801–1809.
- [15] F. El-Moukaddem, E. Torng, G. Xing, Mobile relay configuration in data-intensive wireless sensor networks, *IEEE Trans. Mob. Comput.* 12 (Feb. (2)) (2013) 261–273.
- [16] Z. Liao, J. Wang, S. Zhang, J. Cao, G. Min, Minimizing movement for target coverage and network connectivity in mobile sensor networks, *IEEE Trans. Parallel Distrib. Syst.* 26 (Jul. (7)) (2015) 1971–1983.
- [17] H. Zhang, P. Hong, K. Xue, Mobile-based relay selection schemes for multi-hop cellular networks, *J. Commun. Netw.* 15 (Feb. (1)) (2013) 45–53.
- [18] I. Basturk, B. Ozbek, Effect of mobile relays on the OFDMA-based cellular network performance, in: *Proc. 22nd Signal Process. Commun. Appl. Conf.*, Apr. 2014, pp. 337–340.
- [19] J. Gozalvez, B. Coll-Perales, Experimental evaluation of multihop cellular networks using mobile relays, *IEEE Commun. Mag.* 51 (Jul. (7)) (2013) 122–129.
- [20] H. Nourizadeh, S. Nourizadeh, R. Tafazolli, Performance evaluation of cellular networks with mobile and fixed relay station, in: *Proc. IEEE VTC*, Sept. 2006, pp. 1–5.
- [21] B. Chang, Y. Liang, S. Su, Analyses of relay nodes deployment in 4G wireless mobile multihop relay networks, *Wirel. Pers. Commun.* 83 (Jul. (2)) (2015) 1159–1181.
- [22] B.-C. Min, Y. Kim, S. Lee, J.-W. Jung, E.T. Matson, Finding the optimal location and allocation of relay robots for building a rapid end-to-end wireless communication, *Ad Hoc Netw* 39 (Mar. (15)) (2016) 23–44.
- [23] Z. Liao, X. Zhang, C. Feng, Mobile relay deployment based on Markov chains in WiMAX networks, in: *Proc. IEEE GLOBECOM*, Dec. 2014, pp. 4508–4513.
- [24] Z. Yang, Q. Zhang, Z. Niu, Throughput improvement by joint relay selection and link scheduling in relay-assisted cellular networks, *IEEE Trans. Veh. Tech.* 61 (Jul. (6)) (2012) 2824–2835.
- [25] H. Tang, P. Hong, K. Xue, HeNB-aided virtual-handover for range expansion in LTE femtocell networks, *J. Commun. Netw.* 15 (Jun. (3)) (2013) 312–320.



Hongbin Chen was born in Hunan Province, China in 1981. He received the BEng degree in electronic and information engineering from Nanjing University of Posts and Telecommunications, China, in 2004; and the PhD degree in circuits and systems from South China University of Technology, China, in 2009. He is presently a Professor in the School of Information and Communication, Guilin University of Electronic Technology, China. From October 2006 to May 2008, he was a Research Assistant in the Department of Electronic and Information Engineering, Hong Kong Polytechnic University, China. From March to April 2014, he was a Research Associate in the same department. His research interests lie in energy-efficient wireless communications. He has published more than 50 papers in renowned international journals including *IEEE Transactions*. He is serving as an Editor for *IET Wireless Sensor Systems*.



Wangfeng Chen received a BEng degree in communications engineering from Guangxi Normal University, China in June 2013. She is working towards her MEng degree in Guilin University of Electronic Technology from September 2013. Her research focuses on energy-efficient cellular networks.



Feng Zhao received a PhD degree in communications and information systems from Shandong University, China in 2007. Now he is a Professor in the School of Information and Communication, Guilin University of Electronic Technology, China. His research interests include wireless communications, signal processing, and information security.